Proceedings

Multifunctional Smart Window Based on Dielectric Elastomer Actuator [†]

Milan Shrestha [1],*, Gih-Keong Lau [2], Anand Asundi [3] and Zhenbo Lu [4]

[1] Temasek Laboratories, National University of Singapore, Singapore 117411, Singapore
[2] Department of Mechanical Engineering, National Chiao Tung University, Hsinchu 30010, Taiwan; mgklau@nctu.edu.tw
[3] d'Optron Pte Ltd., 71 Nanyang Avenue, #2M-08, Singapore 638075, Singapore; anandasundi@doptron.com
[4] School of Aeronautics and Astronautics, Sun Yat-Sen University, Guangzhou 510275, China; luzhb7@mail.sysu.edu.cn
* Correspondance: milan001@e.ntu.edu.sg; Tel.: +65-83600602
[†] Presented at the First International Electronic Conference on Actuator Technology: Materials, Devices and Applications, 23–27 November 2020; Available online: https://iecat2020.sciforum.net/.

Abstract: Soft actuators are compliant material-based devices capable of producing large deformations upon external stimuli. Dielectric elastomer actuators (DEAs) are a type of soft actuators that operate on voltage stimuli. Apart from soft robotics, these actuators can serve many novel applications, such as tunable optical gratings, lens, diffusers, smart windows and so on. This article presents our current work on tunable smart windows which can regulate light transmittance and sound absorption. This smart window can promote daylighting while maintaining privacy by electrically switching between being transparent and opaque. As a tunable optical surface scatters, it turns transparent with smooth surfaces like a flat glass; however, it turns opaque (translucent) with the micro-rough surface. The surface roughness is varied, employing surface microwrinkling or unfolding by using dielectric elastomer actuation. In addition, this smart window is equipped with another layer of transparent microperforated dielectric elastomer actuators (DEAs), which act like Helmholtz resonators, serving as a tunable and broader sound absorber. It can electrically tune its absorption spectrum to match the noise frequency for maximum acoustic absorption. The membrane tension and perforation size are tuned using DEA activation to tune its acoustic resonant frequency. Such a novel smart window can be made as cheap as glass due to its simple, all-solid-state construction. In the future, they might be used in smart green building and could potentially enhance urban livability.

Keywords: dielectric elastomer actuators; smart windows; smart acoustic absorbers; transparent thin films; microwrinkling

1. Introduction

Glass panels are widely used as transparent facades for buildings. They are optically transparent to allow daylighting while being acoustic barriers; they isolate the outdoor noise. However, these transparent glasses make the privacy of the buildings vulnerable. In addition, the glass panels are not effective to damp out indoor noise or echoes that reverberate in the events of indoor musical performances or public announcements. Therefore, there is a need for window solutions that can regulate visibility and sufficiently absorb sound as well. Curtains are the simplest solution to achieve both functionalities. Thick textile curtains are often used to block visibility for privacy purposes. They can also act like porous acoustic absorbers to attenuate the indoor noise [1], yet they are unable to provide both functionalities sufficiently and simultaneously. For example, they cannot absorb sound

when they are open to allow daylighting. There are a few translucent sound-absorbing curtains, [2] but they are relatively poor at sound absorption and they still block visibility.

There are different types of glasses which provide either one of these functionalities. For example, there are smart window solutions that can switch between transparent and opaque or translucent as desired. These commercial smart windows are based on electrochromic [3,4], polymer-dispersed liquid crystal (PDLC) devices [5,6] and suspended particle devices (SPDs) [7]. Electrochromic devices in a battery construction change color, and thus the light absorption coefficient, upon electrical stimuli. PDLC devices consist of liquid crystals immersed in a polymer matrix. The random orientations of these liquid crystals are electrically controlled to switch between milky and clear states. An SPD has light-absorbing particles whose distribution is also electrically controlled to adjust the transmission of light. However, these devices are costly to adopt for large-area windows [3]. Their manufacturing cost is high ($200 per square foot) due to complex construction. Besides that, their adoption is hindered by other issues. For example, electrochromic windows are subject to slow responses (taking 5 min to switch a 0.01 square meter panel) and fast aging, whereas PLDC devices and SPDs only show a moderate transparency tuning range (50%–80%) and are not so transparent in their clear states [7]. Moreover, they continuously consume a high amount of power when switched to be transparent. Low-cost transparency switching devices based on a tunable optical diffuser seem promising, but reported devices are far from applicable due to large strain involvement and a narrow tuning range [8–12].

Similarly, there are few transparent glass solutions to minimize the reverberation of indoor noise [13–15]. For example, panel absorbers can be transparent, but they have a narrow absorption frequency bandwidth [16]. Microperforated panel (MPP) absorbers have slightly broader absorption frequency bandwidths, but they are still fixed and unable to absorb sound beyond their absorption bandwidths. These passive absorbers are inefficient when absorbing sound that outlies their absorption bandwidth and are unable to adapt to varying noise frequencies.

Currently, no window appliance can regulate natural daylight in a building, tune the transparency for privacy and sufficiently absorb indoor noise to reduce its reverberation simultaneously at a reasonable price. This article presents a concept of such a low-cost smart window based on dielectric elastomer actuators (DEAs). This work explores the microwrinkling of a hybrid multilayer electrode made of a metal oxide thin film and polymeric conductive thin films. This is used to develop a tunable optical diffuser which requires a low activation strain for transparency switching. This elastomeric, tunable optical diffuser shall meet the stringent requirements for high transmittance in the clear state, a very low transmittance at the translucent state, fast response and long life for repeated cycles. In addition, this work addresses the need for a transparent and tunable broadband acoustic absorber. We used transparent microperforated membranes to make a relative broadband acoustic absorber. In addition, the dielectric elastomer actuator is used to make this absorber tunable. Hence, they can tune their absorption spectrum and maintain optimal absorption of the noise with changing dominant frequencies. Eventually, these two DEA-based components are combined for two functionalities. The first layer provides the transparency switching capability, and the second layer provides tunable broadband noise absorption (see Figure 1b).
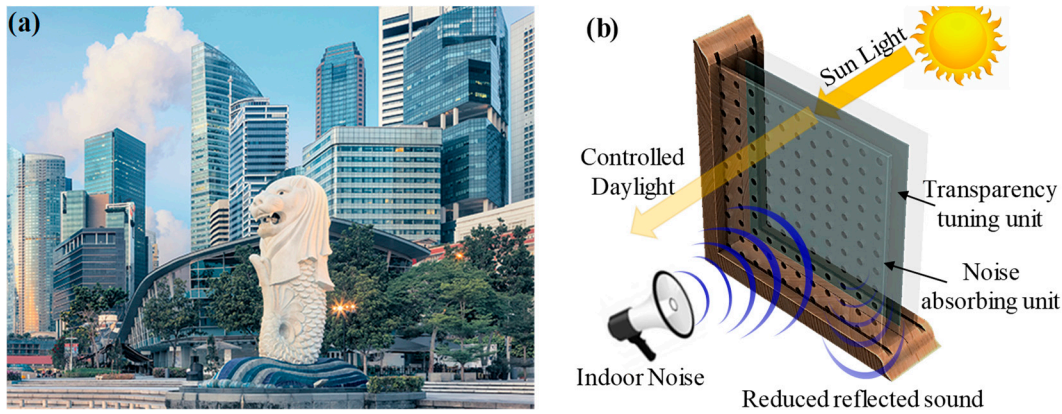
Figure 1. (**a**) The use of many glass facades in most buildings in modern cities. (**b**) Schematic of the smart window made of two components. The first component can tune its transparency, and the second can absorb broadband noise while adapting to the varying noise frequency.

2. Theory

This article presents DEAs for two functionalities. First, it shows a transparency tuning device made of a tunable optical diffuser, consisting of two tunable optical scatterer surfaces sandwiching a dielectric elastomer membrane (see Figure 2a,b). Its surface topography change can tune the scattering of forward visible light [17,18]. For a smooth surface, the total transmittance at a normal incidence is $T = 1 - R = \frac{4n_1 n_2}{(n_2+n_1)^2}$, according to Fresnel equations. Consider a device with two identical Gaussian surfaces of a voltage-tunable roughness σ (V) and finite electrical conductivity. The specular (non-diffuse) part of the total transmittance through the device is expressed as follows [19–21]:

$$T_{spec} = T^2 . \exp\left\{-2\left[\frac{2\pi\sigma(V)}{\lambda}(n_1 - n_2)\right]^2\right\} \tag{1}$$

where $n_1 = 1$ for air and n_2 is greater than 1 for the elastomer substrate. The surface roughens upon the formation of microwrinkles under biaxial compression. Dielectric elastomer actuation can unfold these initially microwrinkled surfaces of compliant electrodes. The application of high voltage V across the dielectric membrane of a thickness t_s induces a compressive electrostatic pressure $P_e = \epsilon_r \epsilon_o (V/t_s)^2$, where ϵ_r is the dielectric constant and ϵ_o is the vacuum permittivity [22,23]. Due to Poisson's ratio effect, the electrostatically squeezed membrane expands in the area. Hence, this voltage-induced areal expansion can reduce the compressive strain in the thin film electrodes. Consequently, it reduces the surface roughness, turning the membrane optically clear.
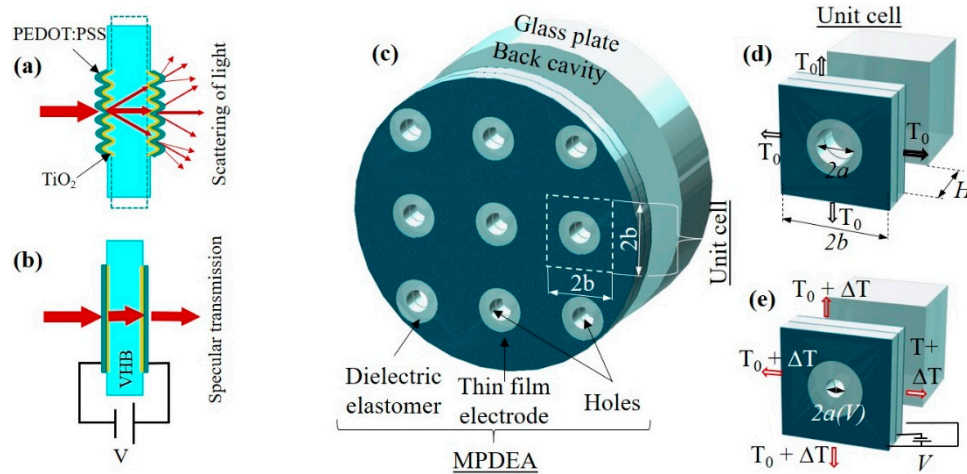
Figure 2. Schematic of the transparency tuning device based on a dielectric elastomer actuator (DEA) optical scatterer. (**a**) The optically scattering state at an inactive state, and (**b**) the optically transparent state at an activated state. (**c**) Schematic of the microperforated dielectric elastomer actuator (MPDEA) device. (**d**) Magnified view of a hole in the MPDEA at an inactive state. (**e**) A hole in the MPDEA at an activated state.

Second, this article presents a smart transparent acoustic absorber, consisting of a microperforated dielectric elastomer actuator (MPDEA) and a 40 mm deep back cavity. The MPDEA consists of a microperforated membrane of a dielectric elastomer sandwiched by a pair of transparent polymeric compliant electrodes. The high voltage activation of the MPDEA reduces the biaxial pre-stress T_0 in the membrane by $\Delta T(V)$ such that the remaining tension becomes

$$T = T_0 - \Delta T(V) = T_0 - \frac{\nu}{1-\nu} P_e \tag{2}$$

where ν is the Poisson's ratio of the dielectric elastomer membrane, according to [24] on the assumption of small elastic strain. Activation of the annular dielectric elastomer that surrounds the passive hole can reduce the hole radius by $\Delta a(V)$, following [25,26]:

$$\Delta a(V) = \frac{\nu}{1-\nu} \frac{P_e}{E} \left[b + \frac{a^2}{b} - 2a - \nu \left(b - \frac{a^2}{b} \right) \right] \tag{3}$$

where b is the half-pitch between the holes (see Figure 2c–e).

A microperforated membrane acoustic absorber can be roughly represented by the unit cells of Helmholtz resonators [27–29]. A Helmholtz resonator is a container of air with a neck-like open hole. When disturbed by the sound, the air in the container or the open hole can vibrate and bounce at a fixed resonant frequency (like a spring–mass system does) to dissipate acoustic energy into heat. According to [29], this resonant frequency of air vibration is determined from the following formula:

$$f = \frac{c}{2\pi} \sqrt{\frac{A}{SL}} \tag{4}$$

where c is the sound speed, A and L are the cross-sectional area and length of the neck-like open hole and S is the volume space of the air container. Here, the hole size (i.e., $A = A(V) = \pi a^2(V)$ and $L = L(V)$) is electrically tunable by a dielectric elastomer actuator [30,31].

3. Experiments

Fabrication of this multifunctional smart window followed the same procedures as making a dielectric electrode actuator. However, the transparency tunable window device used microwrinkled electrodes, [32] which involved the special use of TiO$_2$ and PEDOT:PSS nanometric thin films as the surface scatterer. Fabrication steps included the following (see Figure 3a): (1) biaxially pre-stretching the tape of the acrylate elastomer (3M VHB4905) substrate three times; (2) e-beam evaporation of the

19.8 nm thick TiO$_2$ film; (3) spin coating of a 38.79 nm thick PEDOT:PSS film at 1000 rpm for 1 min (Clevios P Jet HC V2, from Heraeus Deutschland GmbH &f Co. KG); and (4) the optical thin films were radially compressed to form microwrinkles when the elastomer membrane had the pre-stretch partially released from 3.0 times to 2.7 times. Completion of these steps and the membrane transfer to a rigid window frame yielded a complete device, which had aluminium leads to the power supply and electronic instrumentation during testing. The device was subjected to various testing, which included electromechanical activation using a high-voltage power supply (TREK 610E) and measurement for morphology, optical transmittance (using a spectrometer from AvaSpec (USB2 Fiber Optic)) (see Figure 3c) and light scattering using a CMOS sensor of a digital camera (Sony 5100), which was placed at a distance of 20 mm from the device.

Figure 3b shows the fabrication steps for making an MPDEA. First, adhesive tape of acrylate dielectric elastomer (VHB 4910) was pre-stretched radially 3 times to have a 125.0 μm membrane thickness. Later, the pre-stretched membrane was transferred and adhesively bonded to a rigid ring frame of a 20.5 mm internal diameter and a 28 mm external diameter. The pre-stretched elastomer membrane was left for 24 h to relax and let the viscoelastic creep settle to a steady state of deformation. Second, the aqueous conductive ink of the PEDOT:PSS suspension was inkjet printed on the substrate of the pre-stretched membrane. Printing twice and subsequent drying yielded a pair of transparent polymeric compliant electrodes sandwiching the dielectric elastomer membrane. Figure 2c shows a circular electrode of a 20 mm diameter printed on a VHB substrate, except 9 uncoated minor disk areas within it. These 9 uncoated disk areas were arranged in an orthogonal array with equal spacing of $2b = 5$ mm. Finally, a laser cutting machine (Epilog Helix 24) was used to laser drill through the uncoated membrane areas to produce a microperforated DEA (MPDEA). The average diameter of the laser-drilled holes was $2a = 447.5 ± 30.78$ μm. Figure 3d shows an acoustic impedance tube being used to measure the acoustic absorption spectrum of a tunable absorber at normal incidence. The 500 mm long and 20 mm diameter tube had a loudspeaker installed at one end and the tunable absorber mounted at the other end. Two electret array microphones (PCB piezotronic, model 130E20), which were spaced at a 20 mm distance, were used to measure the sound pressure in the tube. In this setup for acoustic testing, a data logger (NI PXI 6221) was used for data recording, while a high-voltage amplifier (Trek model 20/20C) was used for driving the MPDEA device.
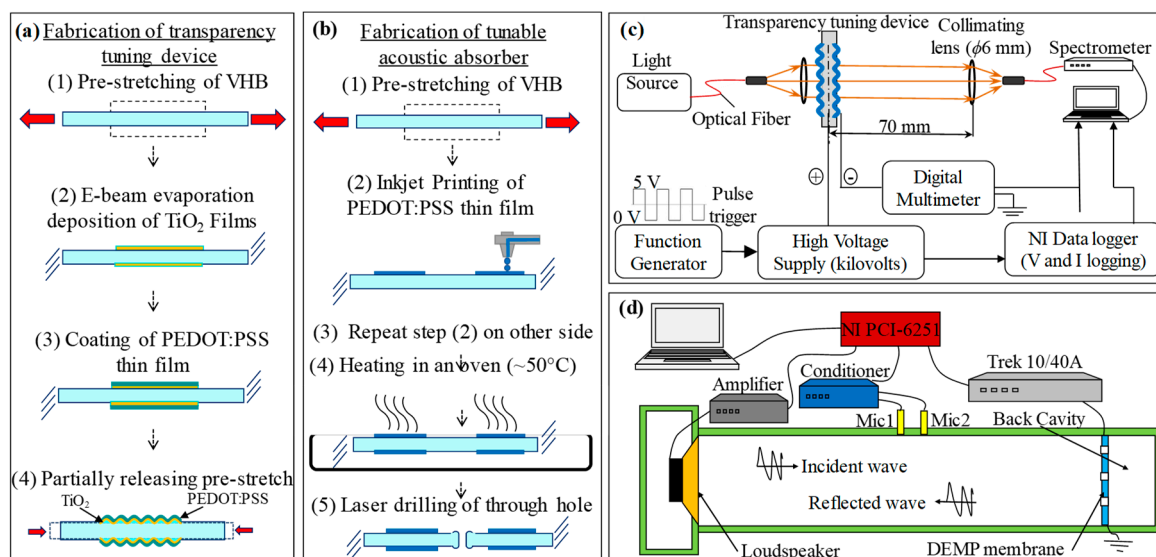
Figure 3. Fabrication procedure of the (**a**) transparency tuning device and (**b**) tunable acoustic absorber, as well as the measurement setup at various activation voltages for (**c**) optical inline transmittance measurement and (**d**) normal acoustic absorption.

4. Results and Discussion

The proposed device consists of two different parallel DEA membranes for two functionalities. The performance of these individual membranes is presented in the following subsections.
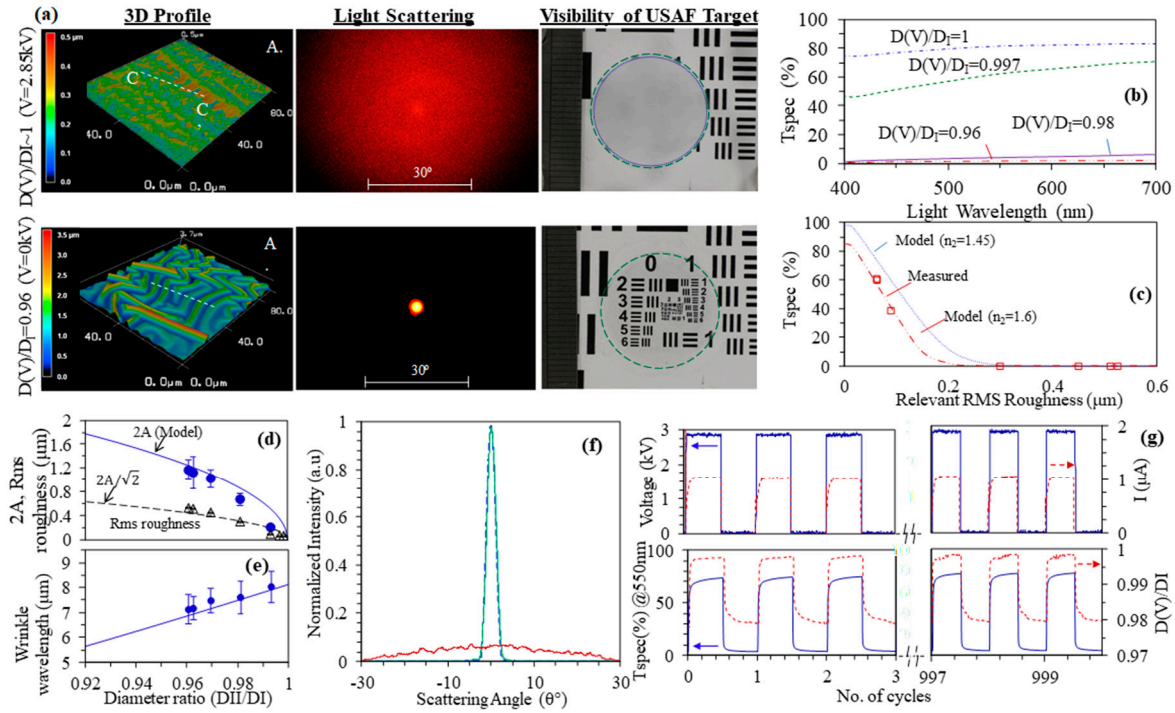
4.1. Transparency Tuning Device

The tested device test was a 45 mm diameter circular dielectric elastomer actuator with 20.0 mm in diameter microwrinkled electrodes. As the elastomer's radial pre-stretch was partially released from 3.0 times to 2.7 times, they buckled the hybrid multilayer thin films into microwrinkles. Figure 4a shows the microwrinkled TiO_2/PEDOT:PSS electrodes in a herringbone pattern under a low precompression of 4–5% strain (D_{II}/D_I = 0.96). Then, the average amplitude of the microwrinkles was 0.585 ± 0.085 μm, while the whole field root mean square (rms) roughness was 0.525 μm. Complete unfolding ($D(V)/D_I$ = 1.0) of the microwrinkled surface could reduce the rms roughness down to approximately 0.036 μm.

Figure 4a–g also shows that the tunable window device could electrically vary the visibility of a logo (i.e., a laser-printed USAF resolution test chart) behind the device. When this tunable device was switched on from 0 kV to 2.85 kV, the diameter ratio increased from $D_{II}/D_I \sim 0.96$ toward 1.0 (see Figure 4g), and thus the microwrinkled surfaces were unfolded. The inline transmittance (for the green light of a 550 nm wavelength) increased from 1.85–3.0% to 78–81%. In addition, the unfolding showed a broadband effect on the increasing specular (inline) transmittance (see Figure 4b). The measured specular transmittance was closely correlated to the rms surface roughness (see Figure 4c). The best fit by Equation (1) to the measurement yielded the determination of an effective refractive index being $n_2 = 1.6$, higher than the $n_2 = 1.47$ of the VHB acrylic elastomer [33]. This enhanced light diffusion confirmed a TiO_2 nanometric film being a stronger surface scatterer than the elastomer substrate. In addition, we measured the angle of light scattering by shining a collimated light beam (of a 635 nm wavelength laser) through this tunable optical diffuser. Figure 4f shows a scattering angle of 44.77° (full width at half of the maximum) at the device's frosted state, but almost no scattering at the device's clear state.

In terms of speed, the switch to clarity took 60 sec (90% rise time), whereas the return to translucence took 2 sec. This suggests that a faster elastic recoil (wrinkling back) takes place at the thin film-coated surface while a slow deactivated creep happens to the bulk viscoelastic elastomer. To demonstrate life-long cyclic switching, we activated and deactivated the window device with a train of high-voltage square pulses (2.85 kV amplitude, 50% duty cycle and a pulse-on width of 1 min) (see Figure 4g). This accelerated test for one thousand cycles confirmed that the TiO_2 interfaces remained intact over repeated cycles of unfolding and wrinkling. At the activated clear state, this window device consumed merely a 0.831 W/m^2 area-specific electrical power despite high-voltage activation. Since it was first prepared four months ago, this tunable window device can still function for long hour activation.
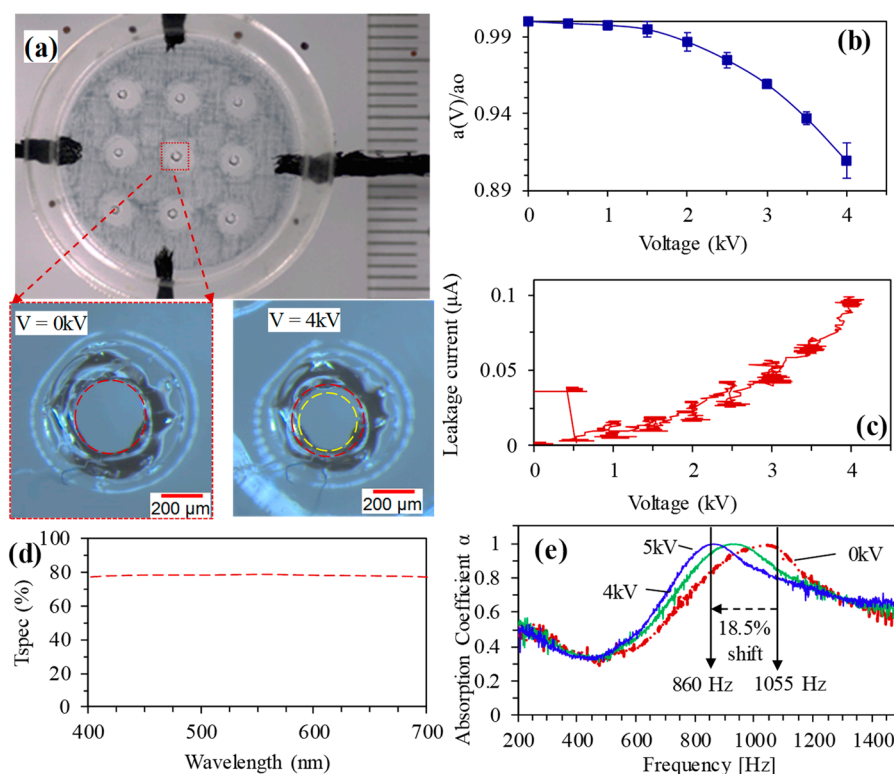
Figure 4. Theoretical and experimental results for the transparency tuning device. (**a**) Surface morphology and consequent light diffusion and visibility of the microwrinkled device. (**b**,**c**) Inline transmittance through the device at various diameter ratios and surface roughness values. (**d**,**e**) Dependence of the surface roughness and wavelength on the diameter ratio of the device. (**f**) Light scattering angle of the device during active (green line) and inactive (red line) states. (**g**) Inline transmittance, diameter ratio and leakage current through the devices at oscillating ON and OFF states for 1000 cycles.

4.2 Tunable Acoustic Absorber

Figure 5a,d shows that MPDEAs with inkjet-printed PEDOT:PSS electrodes are slightly bluish, yet optically clear, with close to 78.64% optical transmittance throughout the visible spectrum. The electrical activation of MPDEAs reduced the perforation hole from an inactivated diameter $2a_o = 447.5 \pm 30.78$ μm to a smaller activated diameter $2a(V)$. The MPDEA can be driven up to 4 kV to reduce the hole diameter by 10%. It consumes 1.27 watt/m^2 of electrical power at the activated state. Figure 5e shows the absorption spectrum of MPDEA-based tunable acoustic absorbers. In the inactivated state, the bandwidth for the above 0.8 acoustic absorption coefficient was 349 Hz (from 831 Hz to 1180 Hz). The peak absorption happened at 1055 Hz upon inactivation (0 kV), but shifted by 18.5% to 860 Hz upon 5.0 kV activation.

Figure 5. Theoretical and experimental results for the tunable window device. (**a**) Front view of the device with magnified views of the holes during active and inactive states. (**b**,**c**) Dependence of the hole diameter and leakage current on the applied voltage. (**d**) Optical transmittance of the device. (**e**) Acoustic spectrum of the device at various activation voltages.

5. Conclusions

This work presented a multi-layered solution for a tunable optical and acoustic window based on dielectric elastomer actuators and transparent wrinkle-capable compliant electrodes. The first layer is for transparency tuning, and its surface roughness is varied, employing surface microwrinkling or unfolding. As small strain-induced microwrinkling and unfolding is desired to make smart glasses, this work showed that the microwrinkling of nanometric films of TiO_2 of a high refractive index was effective to diffuse light down to 1–2% inline transmittance (very frosted) upon a less than 5% axial compressive strain. Interestingly, these brittle oxide thin films can sustain thousands of cycles of microwrinkling and unfolding. A conductive overcoat on the oxide film made of the conductive polymer provides electrical conductivity. Such a multilayer thin film can make a microwrinkled compliant electrode suitable for activating a DEA and thus generate voltage-induced unfolding. Moreover, this device also showed prominent improvements in terms of power consumption (consuming merely ~0.831W/m^2).

The sound-absorbing layer based on a microperforated dielectric elastomer actuator can absorb mid-frequency sound while being optically clear (up to 78.64% light transmission). The need for tuning the resonant frequency to match the noise-dominant frequency can only be addressed using an MPDEA. We devised a mechanism for tuning the hole diameter by the activation of an MPDEA. Unlike other actuators, such as an electric motor or mechanical switches, an MPDEA provides a distributed and quiet actuation. Such novel smart windows can be made as cheap as glass due to their simple, all-solid-state construction. They can be arranged in an array for large area mounting to the window glass. Advances of such transparent tunable acoustic absorbers are anticipated to bring good quality acoustics and natural lighting to indoor spaces.

Author Contributions: M.S., Z.L., A.A. and G.-K.L. conceived the idea and designed the study. M.S. contributed to all the material design and device fabrication. M.S. and Z.L. designed the experimental setup and conducted

the acoustic testing. M.S., Z.L. and G.-K.L. carried out the data analysis. M.S., Z.L. and G.-K.L. derived the models. M.S. wrote the manuscript. All the authors discussed the results and revised the manuscript.

Conflicts of Interest: The authors declare no competing financial interest.

Abbreviations

The following abbreviations are used in this manuscript:

DEA	Dielectric elastomer actuators
MPP	Microperforated panel
MPDEA	Microperforated dielectric elastomer actuator

References

1. Cox, T.J.; D'antonio, P. *Acoustic Absorbers and Diffusers: Theory, Design and Application*; CRC Press: London, UK; New York, NY, USA, 2009.
2. Gerriets-GmbH. Absorber Light. Availabe online: https://www.gerriets.com/us/absorber-light-8172 (accessed on 1 December 2018).
3. Lampert, C.M. Chromogenic smart materials. *Mater. Today* **2004**, *7*, 28–35.
4. Granqvist, C.G. Electrochromics for smart windows: Oxide-based thin films and devices. *Thin Solid Films* **2014**, *564*, 1–38.
5. Doane, J.W.; Vaz, N.A.; Wu, B.G.; Žumer, S. Field controlled light scattering from nematic microdroplets. *Appl. Phys. Lett.* **1986**, *48*, 269–271, doi:10.1063/1.96577.
6. Drzaic, P.S. Polymer dispersed nematic liquid crystal for large area displays and light valves. *J. Appl. Phys.* **1986**, *60*, 2142–2148.
7. Baetens, R.; Jelle, B.P.; Gustavsen, A. Properties, requirements and possibilities of smart windows for dynamic daylight and solar energy control in buildings: A state-of-the-art review. *Solar Energy Mater. Solar Cells* **2010**, *94*, 87–105.
8. van den Ende, D.; Kamminga, J.D.; Boersma, A.; Andritsch, T.; Steeneken, P.G. Voltage-controlled surface wrinkling of elastomeric coatings. *Adv. Mater.* **2013**, *25*, 3438–3442, doi:10.1002/adma.201300459.
9. Görrn, P.; Cao, W.; Wagner, S. Isotropically stretchable gold conductors on elastomeric substrates. *Soft Matter* **2011**, *7*, 7177, doi:10.1039/c1sm05705g.
10. Zang, J.; Ryu, S.; Pugno, N.; Wang, Q.; Tu, Q.; Buehler, M.J.; Zhao, X. Multifunctionality and control of the crumpling and unfolding of large-area graphene. *Nat. Mater.* **2013**, *12*, 321–325, doi:10.1038/nmat3542.
11. Ong, H.-Y.; Shrestha, M.; Lau, G.-K. Microscopically crumpled indium-tin-oxide thin films as compliant electrodes with tunable transmittance. *Appl. Phys. Lett.* **2015**, *107*, 132902, doi:10.1063/1.4932115.
12. Thomas, A.V.; Andow, B.C.; Suresh, S.; Eksik, O.; Yin, J.; Dyson, A.H.; Koratkar, N. Controlled crumpling of graphene oxide films for tunable optical transmittance. *Adv. Mater.* **2015**, *27*, 3256–3265, doi:10.1002/adma.201405821.
13. Kang, J. An acoustic window system with optimum ventilation and daylighting performance. *Noise Vib. Worldw.* **2006**, *37*, 9–17.
14. Asdrubali, F.; Pispola, G. Properties of transparent sound-absorbing panels for use in noise barriers. *J. Acoust. Soc. Am.* **2007**, *121*, 214–221, doi:10.1121/1.2395916.
15. Struiksma, A.; Tenpierik, M.; Snijder, A.; Veer, F.; Botterman, B.; Hornikx, M.; van der Water, H.; Migchielsen, F. Sound absorbing glass: Transparent solution for poor acoustics of monumental spaces. *SPOOL* **2017**, *4*, 53–58.
16. Soundproofing-windows.net. Soundproofing Windows with Double and Triple Glazing. Availabe online: http://soundproofing-windows.net/index.php/soundproofing-windows-with-double-and-triple-glazing (accessed on 1 December 2018).
17. Shrestha, M.; Lau, G.-K. Tunable window device based on micro-wrinkling of nanometric zinc-oxide thin film on elastomer. *Opt. Lett.* **2016**, *41*, 4433, doi:10.1364/ol.41.004433.
18. Shrestha, M.; Asundi, A.; Lau, G.-K. Smart Window Based on Electric Unfolding of Microwrinkled TiO2 Nanometric Films. *ACS Photonics* **2018**, doi:10.1021/acsphotonics.8b00486.

19. Beckmann, P.; Spizzichino, A. *The Scattering of Electromagnetic Waves from Rough Surfaces*; Artech House, Inc.: Norwood, MA, USA, 1987; p. 511.

20. Eastman, J. *Surface Scattering in Optical Interference Coatings*; University of Rochester: New York, NY, USA, 1974.

21. Zeman, M.; van Swaaij, R.A.C.M.M.; Metselaar, J.W.; Schropp, R.E.I. Optical modeling of a-Si:H solar cells with rough interfaces: Effect of back contact and interface roughness. *J. Appl. Phys.* **2000**, *88*, 6436–6443, doi:10.1063/1.1324690.

22. Keplinger, C.; Sun, J.-Y.; Foo, C.C.; Rothemund, P.; Whitesides, G.M.; Suo, Z. Stretchable, transparent, ionic conductors. *Science* **2013**, *341*, 984–987.

23. Lang, U.; Naujoks, N.; Dual, J. Mechanical characterization of PEDOT:PSS thin films. *Synth. Metals* **2009**, *159*, 473–479, doi:10.1016/j.synthmet.2008.11.005.

24. Lau, G.-K.; Heng, K.-R.; Ahmed, A.S.; Shrestha, M. Dielectric elastomer fingers for versatile grasping and nimble pinching. *Appl. Phys. Lett.* **2017**, *110*, 182906, doi:10.1063/1.4983036.

25. Lu, Z.; Shrestha, M.; Lau, G.-K. Electrically tunable and broader-band sound absorption by using micro-perforated dielectric elastomer actuator. *Appl. Phys. Lett.* **2017**, *110*, 182901, doi:10.1063/1.4982634.

26. Shrestha, M.; Lu, Z.; Lau, G.-K. Transparent tunable acoustic absorber membrane using inkjet printed PEDOT: PSS thin-film compliant electrodes. *ACS Appl. Mater. Interfaces* **2018**, doi:10.1021/acsami.8b12368.

27. Maa, D.-Y. Potential of microperforated panel absorber. *J. Acoust. Soc. Am.* **1998**, *104, 2861-2866*.

28. D. Herrin; J. Liu. Properties and applications of microperforated panels. *Sound Vib.* **2011**, *45*, 6–9.

29. Ginn, K. *Architectural Acoustics*; Brüel & Kjaer: Naerum, Denmark, 1978.

30. Shian, S.; Clarke, D.R. Electrically tunable window device. *Opt. Lett.* **2016**, *41*, 1289–1292, doi:10.1364/OL.41.001289.

31. Rosset, S.; Shea, H.R. Flexible and stretchable electrodes for dielectric elastomer actuators. *Appl. Phys. A* **2012**, *110*, 281–307, doi:10.1007/s00339-012-7402-8.

32. Low, S.H.; Lau, G.K. Bi-axially crumpled silver thin-film electrodes for dielectric elastomer actuators. *Smart Mater. Struct.* **2014**, *23*, 125021.

33. 3M. *Converting 3M Technology into Successful Applications*; 3M Industrial Adhesives and Tapes Division: St. Paul, MN, USA, 2015.